British Journal of Pharmacology

DOI:10.1111/j.1476-5381.2011.01658.x
www.brjpharmacol.org

Themed Section: Cannabinoids in Biology and Medicine, Part II

RESEARCH PAPER

Effects of palmitoylation of Cys^{415} in helix 8 of the CB$_1$ cannabinoid receptor on membrane localization and signalling

Sergio Oddi[1,2]*, Enrico Dainese[1,2]*, Simone Sandiford[3‡], Filomena Fezza[2,4], Mirko Lanuti[1,2], Valerio Chiurchiù[2], Antonio Totaro[2], Giuseppina Catanzaro[1,2], Daniela Barcaroli[5], Vincenzo De Laurenzi[5], Diego Centonze[2,6], Somnath Mukhopadhyay[3§], Jana Selent[7], Allyn C Howlett[8†] and Mauro Maccarrone[1,2†]

[1]*Department of Biomedical Sciences, University of Teramo, Teramo, Italy,* [2]*European Center for Brain Research (CERC)/Santa Lucia Foundation I.R.C.C.S., Rome, Italy,* [3]*Neuroscience/Drug Abuse Research Program, Biomedical Biotechnology Research Institute, North Carolina Central University, Durham, NC, USA,* [4]*Department of Experimental Medicine and Biochemical Sciences, University of Rome 'Tor Vergata', Rome, Italy,* [5]*Department of Biomedical Sciences, University of Chieti-Pescara 'G. d'Annunzio', Chieti, Italy,* [6]*Department of Neurosciences, University of Rome 'Tor Vergata', Rome, Italy,* [7]*Research Group of biomedical Informatics (GRIB-IMIM), University of Pompeu Fabra, Barcelona Biomedical Research Park (PRBB), Barcelona, Spain, and* [8]*Department of Physiology and Pharmacology, Wake Forest University Health Sciences, Winston-Salem, NC, USA*

Correspondence
Mauro Maccarrone, Department of Biomedical Sciences, Piazza A. Moro 45, I-64100 Teramo, Italy.
E-mail: mmaccarrone@unite.it

*Equally contributing authors.
†Equally senior authors.
Present addresses: ‡Department of Molecular Microbiology and Immunology, Malaria Research Institute Bloomberg School of Public Health, Johns Hopkins University, Baltimore, MD, USA; §Neuroscience Research Program, Cancer Research Program, Biomedical Biotechnology Research Institute, Department of Chemistry, North Carolina Central University, Durham, NC, USA.

Keywords
drug receptor mechanisms; CB$_1$ cannabinoid receptor; palmitoylation; lipid rafts; receptor trafficking; signalling; GFP-tagged receptors

Keywords
drug receptor mechanisms; CB$_1$ cannabinoid receptor; palmitoylation; lipid rafts; receptor trafficking; signalling; GFP-tagged receptors

Received
29 November 2010
Revised
15 July 2011
Accepted
5 August 2011

BACKGROUND AND PURPOSE

The CB$_1$ cannabinoid receptor is regulated by its association with membrane microdomains such as lipid rafts. Here, we investigated the role of palmitoylation of the CB$_1$ receptor by analysing the functional consequences of site-specific mutation of Cys^{415}, the likely site of palmitoylation at the end of helix 8, in terms of membrane association, raft targeting and signalling.

EXPERIMENTAL APPROACH

The palmitoylation state of CB$_1$ receptors in rat forebrain was assessed by depalmitoylation/repalmitoylation experiments. Cys^{415} was replaced with alanine by site-directed mutagenesis. Green fluorescence protein chimeras of both wild-type and mutant receptors were transiently expressed and functionally characterized in SH-SY5Y cells and HEK-293 cells by means of confocal microscopy, cytofluorimetry and competitive binding assays. Confocal fluorescence recovery after photobleaching was used to assess receptor membrane dynamics, whereas signalling activity was assessed by [^{35}S]GTPγS, cAMP and co-immunoprecipitation assays.

KEY RESULTS

Endogenous CB$_1$ receptors in rat brain were palmitoylated. Mutation of Cys^{415} prevented the palmitoylation of the receptor in transfected cells and reduced its recruitment to plasma membrane and lipid rafts; it also increased protein diffusional mobility. The same mutation markedly reduced the functional coupling of CB$_1$ receptors with G-proteins and adenylyl cyclase, whereas depalmitoylation abolished receptor association with a specific subset of G-proteins.

CONCLUSIONS AND IMPLICATIONS

CB$_1$ receptors were post-translationally modified by palmitoylation. Mutation of Cys^{415} provides a receptor that is functionally impaired in terms of membrane targeting and signalling.

LINKED ARTICLES

This article is part of a themed section on Cannabinoids in Biology and Medicine. To view the other articles in this section visit http://dx.doi.org/10.1111/bph.2012.165.issue-8. To view Part I of Cannabinoids in Biology and Medicine visit http://dx.doi.org/10.1111/bph.2011.163.issue-7

Abbreviations

CB, cannabinoid receptor; CHAPS, 3-([3-cholamidopropyl]dimethylammonio)-1-propanesulfonate; CRAC, cholesterol interaction/ recognition amino acid sequence consensus; DRM, detergent-resistant membrane; FRAP, fluorescence recovery after photobleaching

Introduction

Endocannabinoids exert their biological activity within the CNS and in peripheral tissues mainly by binding to cannabinoid signalling activity signalling activity CB_1 and CB_2 receptors (Howlett, 2005; receptor nomenclature follows Alexander *et al.*, 2011). These proteins belong to the group A GPCRs and represent an emerging class of drug discovery targets with a potential therapeutic value in the modulation of pathophysiological processes and in the treatment of several human diseases (see Pertwee, 2005; Maccarrone, 2006; Di Marzo, 2008). These include modulation of food intake and energy balance (Duncan *et al.*, 2005; Maccarrone *et al.*, 2010), treatment of chronic pain (Cravatt *et al.*, 2001; Cravatt and Lichtman, 2004), anxiety (Kathuria *et al.*, 2003), spasticity (Smith *et al.*, 2010), neurodegenerative (Maccarrone *et al.*, 2007; Scotter *et al.*, 2010) and neuroinflammatory (Centonze *et al.*, 2007) diseases, as well as fertility (Wang *et al.*, 2006) and immune disorders (Klein, 2005).

In the last few years, it has become evident the involvement of membrane lipids, especially cholesterol and glycosphingolipids, in regulating localization and function of GPCRs, such as the β_2-adrenoceptor and the 5-HT_{1A} receptor, as well as of several other membrane-associated proteins such as the caveolins (Pontier *et al.*, 2008; Prinetti *et al.*, 2009; Paila *et al.*, 2010; Shrivastava *et al.*, 2010). Mounting evidence indicates that the CB_1 receptor is dynamically localized and regulated within lipid rafts. In particular, the activity of the CB_1 receptor has been found to depend on membrane cholesterol content and integrity of lipid rafts (Bari *et al.*, 2005; Sarnataro *et al.*, 2005; Oddi *et al.*, 2011). However, the structural determinants responsible for the inc was assessed orporation of the CB_1 receptor into these membrane microdomains are not yet completely identified. Four, not mutually exclusive, mechanisms for raft targeting of a transmembrane protein have been proposed: (i) specific interactions with lipid raft components, such as cholesterol and glycosphingolipids (Eroglu *et al.*, 2003; Pucadyil and Chattopadhyay, 2004); (ii) direct interaction with the scaffolding domain of caveolin (Song *et al.*, 1996; Okamoto *et al.*, 1998); (iii) interaction with hydrophobic amino acids, particularly within the transmembrane domains near the exoplasmic leaflet (Anderson and Jacobson, 2002; Yamabhai and Anderson, 2002); and (iv) the covalent attachment of saturated fatty acyl chains, including myristic and palmitic acids (Milligan *et al.*, 1995; Shaul *et al.*, 1996; Moffett *et al.*, 2000; Zacharias *et al.*, 2002).

We have previously demonstrated that CB_1 receptors directly interact with caveolin-1 (Bari *et al.*, 2008). Very recently, we identified a cholesterol interaction/recognition amino acid sequence consensus (CRAC) (L/V-X[1–5]-Y-X[1–5]-R/K) in the transmembrane helix 7 of CB receptors (Figure 1). By substitution of Lys^{402} of the CB_1 receptor with the Gly present in a corresponding position of CB_2 receptors, we demonstrated a key role of the CRAC sequence in the cholesterol sensitivity of CB_1 receptors, compared with the insensitivity of CB_2 receptors (Oddi *et al.*, 2011).

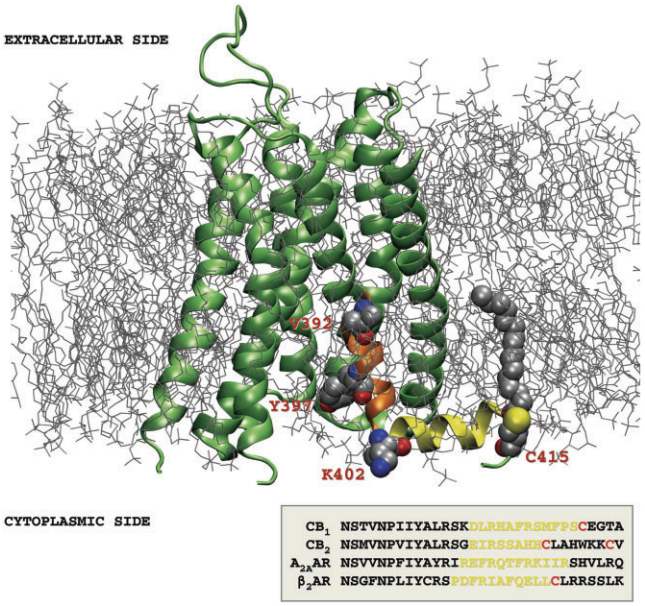

Figure 1

Three-dimensional model of the CB_1 receptor (lime, NewCartoon), based on a sequence alignment with the A_{2A} adenosine receptor (A_{2A}AR) in the activated state (Xu *et al.*, 2011) (PDB code: 3QAK), and embedded within a palmitoyloleoyl-phosphatidylcholine/ cholesterol membrane bilayer. In orange, the region of *trans*-membrane helix 7, containing the CRAC sequence with the relevant residues represented as Van der Waals (VDW) spheres (V392, Y397, K402), is shown. The juxtamembrane C-terminal tail forming helix 8 (yellow) contains the Cys^{415} residue, represented as VDW spheres together with the bound palmitate molecule. The inset at the bottom shows sequence alignment obtained by ClustalW2 programme of the human CB_1, CB_2, A_{2A} receptors and the β_2-adrenoceptor (β_2AR) at the level of helix 8, with the conserved cysteine residues in red. The extracellular loop 2 contains a disulphide bridge between Cys^{257} and Cys^{264} (Fay *et al.*, 2005), represented as VDW spheres. The initial 3-D model of CB_1 receptors was built using the MODELLER software (Sali and Blundell, 1993) and refined by 40 ns molecular dynamics simulation using the ACEMD software (Harvey *et al.*, 2009) as described earlier (Selent *et al.*, 2010).

Another key structural determinant required for membrane binding and lipid raft targeting of transmembrane proteins is palmitoylation (Fukushima *et al.*, 2001; Greaves and Chamberlain, 2007; Greaves *et al.*, 2009). This modification is not essential for raft targeting of proteins. For instance, the transferrin receptor is excluded from rafts despite being palmitoylated (Jing and Trowbridge, 1990) and, under basal conditions, some GPCRs are almost exclusively located in lipid rafts (Navratil *et al.*, 2003) and others are present in these microdomains only in small amounts (Gimpl *et al.*, 1997; Guzzi *et al.*, 2002). Palmitoylation strengthens the association of a protein with plasma membranes, supporting the so-called 'kinetic trapping' theory (Schroeder *et al.*, 1997). This theory implies that palmitoylated proteins have a restricted desorbing ability and thus explains the enrichment of palmitoylated receptors at the level of the plasma membrane (Qanbar and Bouvier, 2003).

Cysteines are by far the most frequent acceptor sites of palmitoylation and 3-D structures of CB_1 receptors obtained by homology modelling with the crystal structures of bovine rhodopsin (Palczewski *et al.*, 2000) revealed the presence of a cysteine residue (Cys^{415}) that is evolutionarily conserved in almost all members of class A GPCRs (Figure 1). Cys^{415} is positioned at the end of the juxtamembrane helix 8, which seems to be critical for receptor activity and regulation and, more notably, is under the influence of the surrounding membrane environment (Tian *et al.*, 2005; Xie and Chen, 2005; Dainese *et al.*, 2010). In rhodopsin, the corresponding cysteine residues Cys^{322} and Cys^{323} are constitutively palmitoylated and so is Cys^{341} in the β_2-adrenoceptor (Figure 1). All these cysteines are supposed to help anchor the C terminal tail of their receptors to cholesterol-rich regions of the membrane (Karnik *et al.*, 1993; Cherezov *et al.*, 2007). Despite mounting experimental evidence demonstrating the modulation of CB_1 receptors by lipid rafts, no information has been yet reported on CB_1 receptor palmitoylation, and on its role in regulating receptor activity and membrane targeting.

In the present study, we demonstrated that majority of CB_1 receptors in rat forebrain are palmitoylated. We also investigated the role of CB_1 receptor palmitoylation by analysing the functional consequences of the site-specific mutation of Cys^{415} at the end of helix 8 (Figure 1), by substituting alanine (mutant CB_1[C415A]-green fluorescent protein [GFP]). We analysed whether this mutation had any effect on various aspects of CB_1 receptor function, including (i) transport to the plasma membrane; (ii) segregation into lipid subdomains; (iii) membrane dynamics; and (iv) coupling to G-proteins and adenylyl cyclase. We performed these functional studies using GFP, which allowed us to assay the biological properties of the receptor also at a single-cell resolution. GFP chimeras of both wild-type and mutant CB_1 receptors were transiently expressed in HEK-293 cells or in human neuronal SH-SY5Y cells. We found that mutation of Cys^{415} led to reduced recruitment of the receptor both on the cell surface and within lipid rafts. Using the technique,of fluorescence recovery after photobleaching (FRAP), we showed that the C415A mutant had an increased diffusional mobility within the plasma membrane. Finally, we found that the substitution of Cys^{415} by alanine reduced the functional coupling of CB_1 receptor with G-proteins and adenylyl cyclase, both in the presence and in the absence of a CB_1 receptor agonist. In line with these data, we demonstrated that palmitoylation/depalmitoylation can modify the CB_1 receptor interaction with G-proteins. In summary, our data demonstrate that palmitoylation of Cys^{415} played critical roles in the spatio-functional regulation of CB_1 receptors.

Methods

Radioactive palmitoylation assay

Plasma membrane-enriched P2 membranes were prepared from rat forebrains, as previously described (Beck *et al.*, 2002). To determine the palmitoylation state of CB_1 receptors in rat forebrain, P2 membranes (10 $mg \cdot mL^{-1}$) were either depalmitoylated with 1 M hydroxylamine (30 min at 37°C) to break thioesters (Linder *et al.*, 1993; Loisel *et al.*, 1996) or were left untreated (control). The treated and control membranes were washed and then incubated with [^{3}H]palmitoyl-CoA (20 μM) for 30 min at 37°C. Membranes were solubilized with 3-([3-cholamidopropyl]dimethylammonio)-1-propanesulfonate (CHAPS) and immunoprecipitated with a CB_1 receptor antibody against the N-terminal 14 amino acids (Howlett *et al.*, 1998) and proteins were separated by SDS-urea-PAGE, as reported by Mukhopadhyay and Howlett, (2005). Each lane was cut into 5 mm slices and radioactivity in the fraction coinciding with the CB_1 receptor was quantitated by liquid scintillation counting.

GFP fusion constructs and site-directed mutagenesis

To generate GFPs, human CB_1 receptor was amplified and cloned in-frame to a GFP-tag in a pVL-GFP vector (AB Vector, San Diego, CA, USA). The CB_1(C415A)-GFP receptor mutant was generated by site-directed mutagenesis with the Quikchange Multi-Site Direct Mutagenesis kit (Stratagene, Rome, Italy), according to the manufacturer's protocol. The primers used were 5′- AGCATGTTTCCCTCTGCTGAAGGCACTGCG CAGC –3′ and 5′- GCTGCGCAGTGCCTTCAGCAGAGGGA AACATGCT –3′.

Cell culture and transfection

N18TG2, SH-SY5Y neuronal cells and HEK-293 cells were grown in DMEM/HF12 or RPMI culture medium, respectively, supplemented with 10% fetal bovine serum or heat-inactivated calf serum, glutamine, sodium pyruvate, penicillin and streptomycin, at 37°C in a 5% CO_2 humidified atmosphere (Mukhopadhyay and Howlett, 2005; Oddi *et al.*, 2011). Cell lines were used at low passage numbers: 15–35 for N18TG2, 20–40 for SH-SY5Y and 25–45 for HEK-293. Monolayers of native cells at 70–80% confluence in 100 mm plates, eight-well chamber slides (Ibidi, Milan, Italy) or in collagen-coated (20 $\mu g \cdot mL^{-1}$) cover slips (10 mm diameter) were transiently transfected with CB_1-GFP or CB_1(C415A)-GFP receptors, using the Attractene reagent as suggested by the manufacturer (QIAGEN, Milan, Italy).

Non-radioactive palmitoylation assay

Labelling of *S*-palmitoylated residues with biotin-tags was carried out as described previously (Drisdel *et al.*, 2006) with

minor modifications. Briefly, membranes of transfected HEK-293 cells expressing the wild-type or mutant receptors were prepared as reported (Bari *et al.*, 2008), and were incubated overnight at 4°C in PBS containing 50 mM *N*-ethylmaleimide, in order to block all pre-existing free sulfhydryls. Membranes were washed and treated with 1 M hydroxylamine (pH 7.4) at room temperature, to cleave the thioester bond and to expose reactive cysteines by detaching the palmitic acid. As a negative control, equal amounts of membranes were treated with 1 M Tris-HCl (pH 7.4). Subsequently, membranes were washed and incubated with 10 μM 1-biotinamido-4-(4′-[maleimidoethyl-cyclohexane]-carboxamido)butane (pH 7.4) at 4°C for 1 h, to label reactive cysteine residues. After three washes, membranes were lysed in 50 mM Tris-HCl (pH 7.4) buffer, containing 150 mM NaCl, 5 mM EDTA and 1% Triton X-100. GFP-tagged receptors were immunoprecipitated using μMACS™ GFP Isolation Kit (Miltenyi Biotec, Milan, Italy), and were eluted with hot (95°C) loading buffer. Following SDS-PAGE and transfer to nitrocellulose membranes, the blots were reacted with streptavidin-horseradish peroxidase (HRP) to detect biotin-labelled proteins. The blots were reprobed with anti-CB_1 receptor antibody to reveal the immunoprecipitated receptors.

Western blotting

Transfected cells were lysed with buffer L (50 mM Tris-HCl, pH 7.4, 150 mM NaCl, 1 mM $MgCl_2$, 1 mM EDTA, 1% Triton X-100, 10% glycerol), and were centrifuged for 20 min at 18 000× *g* at 4°C. The supernatants were recovered and the protein concentration measured through the Bradford assay. Cell homogenates (50 μg·lane^{-1}) were subjected to 12% SDS-PAGE under reducing conditions, then gels were electroblotted onto 0.45 μm nitrocellulose filters (Whatman, Springfield Mill, UK) and were immunoreacted with rabbit anti-CB_1 polyclonal antibodies (1:400, Abcam, Cambridge, UK) and rabbit anti-actin (1:10 000; Sigma Chemical Co.). Goat anti-rabbit-HRP (1:10 000, Santa Cruz Biotechnologies, Santa Cruz, CA, USA) was used as secondary antibody. Blots were developed using the ECL plus system (Amersham Biosciences, Piscataway, NJ, USA), and band densitometry was performed using ImageJ software (National Institutes of Health, Bethesda, MD, USA).

FACS analysis

The total expression of GFP-tagged wild type and mutant CB_1 receptors was confirmed in SH-SY5Y and HEK-293 cells by flow cytometry 48 h after transfection,. Samples were excited at 488 nm and emitted fluorescence was detected through a 515–540 nm band pass filter. FlowJo software (Treestar, Ashland, OR, USA) was used to analyse the expression levels of 10 000 cells, by determining the mean intensity of the GFP fluorescence per cell.

For assaying cell surface expression of the receptors, cells (5×10^5) were collected 48 h after transfection, washed twice with PBS and stained firstly with PA1-745 anti-CB_1 receptor polyclonal antibody (Affinity Bioreagents, Milan, Italy), and then with allophycocyanin (APC)-conjugated secondary antibody (Alexa-fluor 633, Invitrogen, Molecular Probes, Milan, Italy), both dissolved in PBS with 0.5% FBS and 0.02% NaN_3. Surface expression of CB_1 receptors was analysed by FACS-Canto (Becton Dickinson, Milan, Italy), gating on GFP-FITC positive cells (Oddi *et al.*, 2011). The mean channel fluorescence was used to compare the levels of receptor expression at the plasma membrane. Data were corrected by subtracting the non-specific APC fluorescence obtained for GFP-transfected cells, and were analysed by FlowJo software.

Confocal imaging

A Leica TCS SP5 DMI6000 confocal microscope (Leica Microsystems, Wetzlar, Germany) was equipped with HCX plan apo 40× (numerical aperture 1.25) or 63× (numerical aperture 1.4) oil immersion objectives. Excitation laser lines were 488 nm (argon laser) and 561 nm (diode-pumped solid state laser). GFP-tagged receptors were excited at 488 nm and the corresponding fluorescence was detected using a 525 ± 25 nm bandpass filter. Red fluorophores (Alexa Fluor 555-conjugated cholera toxin subunit B and $DiIC_{16}$) were excited using a 561 nm laser line and the corresponding fluorescence was detected using a 580–620 nm bandpass filter. In the co-detection experiments of GFP and red fluorophores, cells were fixed and green fluorescence emission and red fluorescence emission were acquired sequentially upon excitation with 488 nm and 561 nm laser light respectively. Pictures were taken using the LAS AF software (Leica Microsystems). For presentation purposes, LAS AF pictures were exported in TIFF format and processed with Adobe Photoshop CS2 (Mountain View, CA, USA), for adjustments of brightness and contrast.

For the *in situ* detergent extraction assay, Triton X-100 solubilization was performed as described previously (Nichols *et al.*, 2001). Briefly, transfected cells were labelled with Alexa Fluor 555-conjugated cholera toxin subunit B, as suggested by the manufacturer (Invitrogen). Detergent extraction was performed by incubating cells with 1% Triton X-100 in phosphate-buffered saline (PBS) at 4°C for 30 min. After treatment, cells were extensively washed with PBS, fixed with 3% paraformaldehyde in PBS for 20 min at room temperature, mounted using the antifade Prolong Gold reagent, and then visualized by confocal microscopy.

For image analysis, five fields from at least three independent experiments were examined for each treatment. Quantification of the mean fluorescence intensity in selected regions was carried out using ImageJ software (http://rsb.info.nih.gov/ij/).

For quantification of the membrane targeting of GFP-tagged CB_1 receptors, we imaged transfected cells that were co-stained by extracellular application of the red emitting lipophilic dye $DiIC_{16}$ (Oddi *et al.*, 2011). Briefly, transfected cells were washed three times with RPMI without phenol red, incubated with RPMI containing 4 μg·mL^{-1} $DiIC_{16}$ for 5 min on ice, rinsed twice with cold PBS, fixed with 2% formaldehyde in PBS, and examined by confocal fluorescence imaging. The level of localization of GFP-tagged CB_1 receptors at the cell surface was obtained by measuring the degree of overlap between red ($DiIC_{16}$) and green (GFP-tagged receptors) fluorescence (Marchant *et al.*, 2002). These analyses were restricted to the plasma membrane regions (measured from the edge of the cell to 300 nm inside), and data from high-resolution images of 20–30 cells from two to three independent experiments were acquired.

For co-localization analysis, we determined the Pearson's correlation coefficient and the intensity correlation quotient, by using the ImageJ plugin JACoP software, that groups together the most utilized co-localization tools (Bolte and Cordelieres, 2006). Values for Pearson's correlation coefficient can range from +1 to −1: +1 represents a perfect correlation, −1 represents a perfect exclusion, and 0 represents a random localization (Manders *et al.*, 1993). In addition, apparent co-localization due to random staining, or very high intensity, in one window will have values of intensity correlation quotient near to zero, while if the two signal intensities are interdependent (co-localized) these values will be positive with a maximum of 0.5 (Li *et al.*, 2004).

FRAP measurements

For FRAP experiments, 24 h after transfection the chamber slides were held at 37°C on the confocal microscope stage, equipped with an HCX plan apo 63× oil immersion objective. GFP fluorescence was monitored with a digital zoom of 1.2, at a rate of 400 Hz, using an excitation wavelength of 488 nm and a 500–600 nm emission range. The fluorescent periphery of cells represents the plasma membrane, and was selected for bleaching and for monitoring the recovery of fluorescence (Oddi *et al.*, 2011). Each FRAP experiment started with taking five pre-bleach images (0.6 s·frame^{-1}) at low laser intensity (2%), followed by bleaching of a circular region of interest (4 μm diameter) by means of five scans with the 488 nm laser line at full power; then, fluorescence recovery was monitored by taking 600 images (155 ms·frame^{-1}) at low (2%) laser intensity. Loss of fluorescence due to scanning during the FRAP protocol was never larger than 12%. To build up FRAP curves, the fluorescence intensities were background-subtracted (choosing a cell-free area), and were corrected for fluorescence fading during scanning by dividing by the control region intensity; data were then normalized to pre-bleach values. Non-linear regression fitting of each data set, derived from an average of nine experiments, was obtained using the following function that describes the diffusional recovery into circular regions:

$$F(t) = A \cdot e^{-2T/t} \cdot (I_0(2T/t) + I_1(2T/t)) + B$$

where F(t) is the mean background-corrected and normalized fluorescence intensity at time t in the membrane region within the bleached region; I_0 and I_1 are modified Bessel functions; B sets the fluorescence directly after the bleaching; and A + B determines the saturation value of the recovery. The typical recovery time (T) was used to determine the diffusion coefficient (D):

$$D = r^2/(4 \cdot T)$$

where r is the radius of the circular beam. The mobile fraction (M_f) was calculated according to the equation:

$$M_f = (F_\infty - F_0)/(F_i - F_0)$$

where F_∞ is the fluorescence in the bleached region after full recovery; F_i is the fluorescence before bleaching and F_0 is the fluorescence just after the bleach. The immobile fraction (I_f), that is the fraction of immobilized receptor molecules that are not free to diffuse out of the bleached area over the time course of the experiment, was calculated by the equation:

$$If = 1 - Mf$$

Receptor binding assay

For cannabinoid receptor binding studies, cells were collected 48 h after transfection and plated onto 24-well plates. The cells were washed twice with 0.5 mL PBS and were incubated with [^{3}H]CP55940 (0.5–20 nM) in assay buffer (50 mM HEPES, pH 7.4, 1 mM $MgCl_2$, 1 mM $CaCl_2$, 0.2% BSA) for 1 h at 30°C. Incubations were stopped by aspirating the media and then the wells were washed twice with 0.5 mL of ice-cold wash buffer (50 mM HEPES, pH 7.4, 500 mM NaCl, 0.1% BSA). In all binding experiments, nonspecific binding was determined in the presence of 20 μM CP55490.

[^{35}S]GTPγS binding assay

For [^{35}S]GTPγS binding assays, cells were collected 48 h after transfection and plated onto 24-well plates. The binding experiments were performed on whole cells essentially as described (Bari *et al.*, 2005). Briefly, cells were rinsed twice for 5 min at 37°C with 0.5 mL per well wash buffer (50 mM Tris–HCl, pH 7.4, 1 mM $MgCl_2$, 0.2 mM EGTA, 100 mM NaCl), then they were incubated for 2 min at room temperature in 0.5 mL per well saponin solution (140 mM potassium glutamate–HCl, pH 6.8, 1 mg·mL^{-1} ATP, 0.1 mg·mL^{-1} saponin), in order to achieve permeabilization. The cells were pre-incubated in 4 mU·mL^{-1} adenosine deaminase (183 units·mg^{-1} of protein, Sigma Chemicals Co.) for 10 min at 30°C. The binding of [^{35}S]GTPγS stimulated by various amounts of CP55940 was assayed in the presence of 100 μM guanosine diphosphate and 0.1 nM [^{35}S]GTPγS in assay buffer (50 mM Tris-HCl, pH 7.4, 3 mM $MgCl_2$, 1 mM EGTA) in a final volume of 0.5 mL. Non-specific binding was determined in the absence of agonist and in the presence of 30 μM unlabeled GTPγS.

cAMP assay

CB_1 receptors are functionally coupled to $G\alpha_{i/o}$ proteins, and exert a high basal constitutive inhibition of adenylyl cyclase (Bouaboula *et al.*, 1997; Leterrier *et al.*, 2004). The effect of the absence or presence of the CB_1 receptor agonist CP55940 on the forskolin-stimulated accumulation of cAMP in intact transfected cells was determined with the LANCE ULTRA cAMP kit (Perkin Elmer, Rome, Italy), according to the manufacturer's instructions. Briefly, 24 h after transfection, cells were collected and incubated for 30 min with 1 mM 1-methyl-3-isobutylxanthine; then, 0.45 μM forskolin was added in the presence or absence of various amounts of CP55940 (10^{-10}–10^{-4} M). Cells were incubated for 30 min at 37°C, and the reaction was stopped by adding the lysis buffer of the kit. Time-resolved fluorescence was measured with a Victor V Multilabel counter (Perkin Elmer).

Co-immunoprecipitation assays

Membrane fractions were prepared from N18TG2 neuronal cells, as previously described (Mukhopadhyay and Howlett, 2005). P2 membrane fractions from rat forebrains or N18TG2

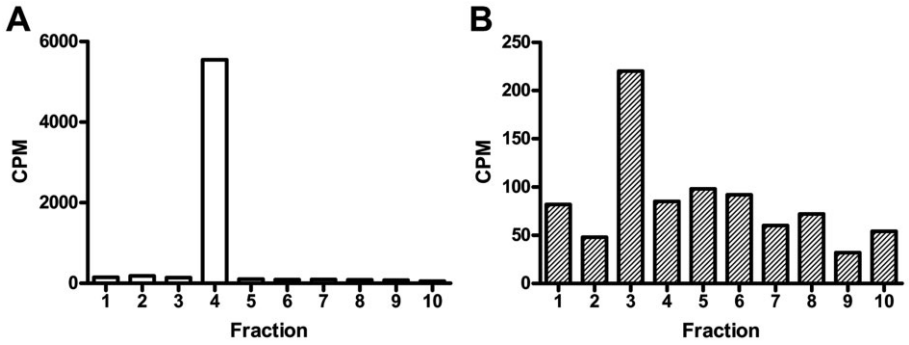

Figure 2

Back-repalmitoylation of brain CB_1 receptors. Rat brain membrane proteins (10 mg·mL^{-1}) were depalmitoylated by incubating the membranes with 1 M hydroxylamine (30 min at 37°C). Treated and control membranes were washed, and then were incubated with [^{3}H]palmitoyl-CoA (20 μM, 30 min at 37°C). Membranes were CHAPS-solubilized and immunoprecipitated with an anti-CB_1 receptor antibody. They were then analysed bySDS-urea-PAGE, and lanes were sliced in 5 mm slices for liquid scintillation counting. The histogram represents the back-palmitoylated cpm obtained from (A) depalmitoylated and (B) control membranes. 1: top of gel; slice 4 coincides with CB_1 receptor immunoreactivity. Note differences in Y-axis scale.

cells (10 mg·mL^{-1}) were depalmitoylated in HME buffer (50 mM HEPES, pH 7.4; 5 mM $MgCl_2$, 5 mM EDTA) containing 100 μM hydroxylamine for 20 min at 4°C, sedimented and washed twice with HME buffer. For repalmitoylation, control or depalmitoylated membranes in HME buffer were treated with 20 μM palmitoyl-CoA for 30 min at 37°C (Duncan and Gilman, 1996). Following these treatments, membrane proteins (5 mg) were sedimented at 17 000× *g*, and resuspended in 500 μL solubilization buffer (30 mM Tris-HCl, pH 7.4; 5 mM $MgCl_2$; 8 mM CHAPS; 20% glycerol), as reported (Houston and Howlett, 1993). CHAPS-solubilized proteins were immunoprecipitated with CB_1 receptor antibody, and Western blots were performed on SDS-urea-10% PAGE. Detection was performed with N-terminal CB_1 receptor antibody and antibodies specific for $G\alpha_{i2}$, $G\alpha_{i3}$ or $G\alpha_o$ (Biomol, Plymouth Meeting, PA, USA) as described (Mukhopadhyay and Howlett, 2005).

Statistical analysis

Data reported in this paper are the means ± SEM of at least two independent experiments, each performed in triplicate. Statistical analysis was performed by using unpaired Student's *t*-test or one-way ANOVA with Newman–Keuls post-test for computing *P*-values. All measurements were plotted and analysed using Graph Pad Prism 5 software (GraphPAD Software, San Diego, CA, USA).

Materials

All chemicals were of the purest analytical grade. [^{3}H]CP55940 (126 Ci·mmoL^{-1}) and [^{35}S]GTPγS (1250 Ci·mmoL^{-1}) were purchased from Perkin-Elmer Life Sciences, Inc. (Boston, MA, USA). Alexa Fluor 555-conjugated cholera toxin subunit B, DiIC16 and Prolong Gold anti-fade kit were purchased from Molecular Probes (Eugene, OR, USA). *N*-Ethylmaleimide or 1-biotinamido-4-(4′-[maleimidomethyl] cyclohexanecarboxamido) butane were purchased from Pierce (Rockford, IL, USA). Attractene was from QIAGEN (Milan, Italy). Culture media, sera and supplements were from Euroclone (Milan, Italy) or Gibco (Grand Island, NY, USA). All other chemicals were purchased from Sigma Chemical Co. (Milan, Italy), unless stated otherwise.

Results

CB_1 receptors are palmitoylated in rat forebrain

To assess the basal palmitoylation state of CB_1 receptors *in vivo*, we performed 'back-palmitoylation' experiments to demonstrate that the majority of rat brain CB_1 receptors exist in the palmitoylated form (Figure 2). The amount of [^{3}H]palmitoylated CB_1 receptor found in the untreated versus treated membranes indicated that >95% (i.e. 5500 cpm in the CB_1 receptor band vs. 225 cpm in the non-depalmitoylated CB_1 receptor band) of these receptors exist in the palmitoylated form in the crude membrane fraction.

Cys^{415} is the main site for CB_1 receptor palmitoylation

Then, we investigated whether the CB_1 receptor was palmitoylated at its Cys^{415} residue in helix 8, by generating the alanine substitution mutant CB_1(C415A)-GFP. This recombinant receptor and the CB_1-GFP controls were expressed in human neuronal SH-SY5Y cells (Figure 3). Our previous studies demonstrated that the fusion of GFP to the C-terminal of CB_1 receptors generates a functional chimeric protein with properties comparable with those of the untagged receptors (Oddi *et al.*, 2011). Due to the low expression (<1 pmol·mg^{-1} protein) of both receptors in SH-SY5Y cells, it was impossible to demonstrate that CB_1 receptors were palmitoylated by directly measuring [^{3}H]palmitate incorporation (data not shown). Thus, we used HEK-293 cells because of the much higher efficiency of receptor transfection in these cells. We also found that in HEK-293 cells, transient transfection of the constructs led to expression levels of

fmol·mg^{-1} of proteins, as assessed by radioligand binding assays. Such a low expression level prevented the assessment of the palmitoylation state of the mutant receptor through a metabolic labelling with radioactive palmitate (Chen *et al.*, 1998; Drisdel *et al.*, 2004). For this reason, we used an alternative methodology, based on the exchange of the fatty acid group at the site of palmitoylation with biotin, which is more readily detected via Western blotting. Using this approach on transiently transfected HEK-293 cells, an increased incorporation of biotin-tags was observed for the wild-type receptor following treatment with hydroxylamine, demonstrating that the wild-type CB_1 receptors were palmitoylated (Figure 3). However for the mutant receptor, no increase in biotin labelling following hydroxylamine treatment was found, demonstrating that the wid-type CB_1 receptor was selectively palmitoylated at Cys^{415} (Figure 3).

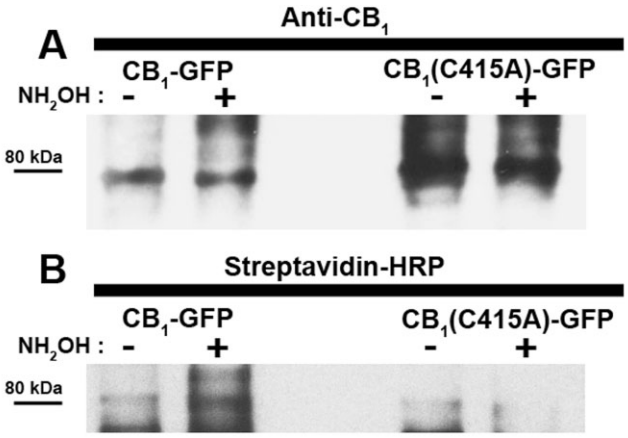

Figure 3

Palmitoylation state of human CB_1-GFP receptor. CB_1-GFP and CB_1-(C415A)-GFP were transiently expressed in HEK-293 cells and their palmitoylation state was assessed by the acyl-biotin exchange reaction (see Methods for more details). (A) As control for the levels of the immunoprecipitated receptors, CB_1-GFP and CB_1-(C415A)-GFP labelled with 1-biotinamido-4-[4′-(maleididomethyl) cyclohexanecarboxamido] butane after incubation in the absence (–) or presence (+) of hydroxylamine (NH_2OH), was immunodetected with anti-CB_1 receptor antibody (anti-CB_1). (B) Biotin-labelled receptors (i.e. palmitoylated receptors) were visualized by probing the same membrane (after stripping) with streptavidin-HRP. Results are representative of two independent experiments.

CB_1-GFP and CB_1(C415A)-GFP receptors are expressed with similar efficiency

It is widely accepted that changing the level of cellular expression of a receptor can have a significant impact on its trafficking and function. Thus, to directly compare the biological properties of wild-type CB_1 receptors and of the C415A mutant, an essential prerequisite is that both receptors have similar expression levels. The cellular amount of CB_1 and CB_1(C415A)-GFP receptors expressed in SH-SY5Y cells was analysed by Western blotting and flow cytometry (Figure 4). As shown in Figure 4A, wild-type and mutant receptors exhibited similar levels of expression, suggesting that the C415A point mutation did not affect the apparent expression or stability of the receptor (Figure 4A). Consistent with the immunoblotting results, cells expressing CB_1-GFP or CB_1(C415A)-GFP receptors exhibited a comparable mean GFP fluorescence per cell (Figure 4B). Similar results were obtained when CB_1 and CB_1(C415A)-GFP receptors were expressed in HEK-293 cells (data not shown).

Next, we addressed the role played by Cys^{415} in various aspects of CB_1 receptor function, such as subcellular distribu-

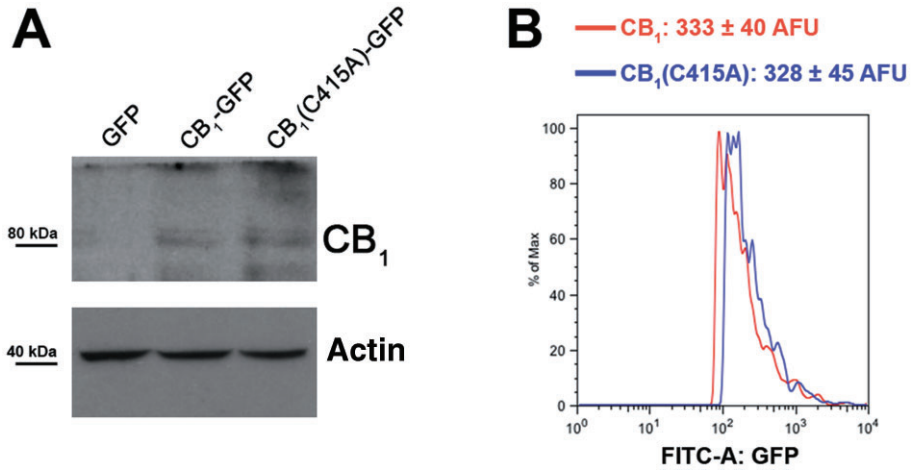

Figure 4

Evaluation of the expression efficiency of CB_1-GFP and CB_1(C415A)-GFP receptors. (A) CB_1-GFP or CB_1(C415A)-GFP expression vectors were transiently transfected into SH-SY5Y cells, and their expression levels were analysed by Western blotting of whole cell lysates using an anti-CB_1 receptor antibody. (B) Histogram plots showing green fluorescence exhibited by SH-SY5Y cells transfected by the same constructs. Twenty-four hours after transfection, cells were trypsinized and analysed for GFP expression by FACS. More details are given under Methods. Results are expressed as mean ± SEM and are representative of two independent experiments.

tion, dynamics and signalling, all of which are known to be modulated by palmitoylation in other GPCRs (Chini and Parenti, 2009).

Cys^{415} is involved in targeting CB$_1$ receptors to the plasma membrane

In order to determine whether the C415A mutation could alter CB_1 receptor membrane targeting, we imaged transfected cells that were co-stained with $DiIC_{16}$, a red fluorescent lipid probe that selectively labels the plasma membrane. Then, the evaluation of the extent of localization of CB_1-GFP and CB_1(C415A)-GFP receptors at the cell surface of SH-SY5Y cells was performed by measuring the degree of overlap of the fluorescence signals. Compared with the wild-type receptor, CB_1(C415A)-GFP receptor showed a reduced localization on the plasma membrane (Figure 5A–F, and Table 1). In order to exclude the possibility that the difference in the intracellular distribution of wild-type and mutant receptors might be due to a different expression level within the observed cells, we tested whether the localization within the plasma membrane depended on the receptor expression level. To this end, for each receptor, we analysed 100 cells, quantifying the mean GFP green fluorescence (that represents the expression level in the cell) and the overlap coefficient (that represents the degree of overlap between the receptor and the membrane probe) (Figure 5G and H). The resulting graphs for each receptor showed that there was no correlation between the expression level of the receptors and their membrane localization, because both the correlation coefficients were very low ($R^2 < 0.005$) and the slopes of the correlation were weakly negative and not significantly different from zero; overall, these parameters showed that the overlap coefficients did not vary with the mean cell fluorescence for both wild-type and mutant receptors.

Membrane targeting of the GFP-tagged receptors was further analysed by FACS analysis. To this end, live cells expressing wild-type and mutant CB_1 receptors were labelled with PA1-745, a polyclonal antibody that recognizes the N-terminal domain of CB_1 receptors. As shown in Figure 5K, mutation of C415 significantly reduced cell surface localization of the CB_1(C415A)-GFP receptor ($P < 0.01$). Interestingly, among the CB_1-transfected cells, less than 20% expressed the wild-type CB_1 receptors on the plasma membrane at an appreciable level and this proportion was lower in cells transfected with CB_1(C415A)-GFP (Figure 5I and J, $P < 0.01$).

Cys^{415} plays a role in the interaction of CB$_1$ receptors with lipid rafts

Next, we compared the association of CB_1-GFP and CB_1(C415A)-GFP receptors with lipid rafts by using *in situ* extraction of transfected cells with Triton X-100, a method that has been previously applied to investigate detergent resistance of the 5-HT_{1A} receptor (Kalipatnapu and Chattopadhyay, 2004). As a control, transfected SH-SY5Y cells were co-stained with cholera toxin B-Alexa Fluor 555, a fluorescent probe that specifically binds the raft constituent ganglioside GM_1, forming a choleragen-ganglioside complex that is resistant to detergent extraction (Hagmann and Fishman, 1982). As expected, ~80% of the cholera toxin B was found to resist Triton X-100 extraction (Figure 6A). We have previously shown that a small but significant pool (~20%) of CB_1-GFP receptor remained associated with detergent-resistant membrane (DRM) remnants after Triton X-100 extraction (Oddi *et al.*, 2011). Here, we found a small, although not significant, reduction in the DRM-confined fraction of the mutant receptor (Figure 6A and Table 1). More significantly, when we analysed the subcellular localization of receptor fluorescence after detergent extraction, we found that a substantial pool of the DRM-associated CB_1 receptor was confined to the plasma membrane, whereas the amount of CB_1(C415A)-GFP receptor on the cell surface was markedly reduced, as measured by the degree of overlap between CB_1 and $DiIC_{16}$ (Figure 6B and Table 1, $P < 0.001$). To further investigate the physical interaction of the two receptors with sphingolipid/cholesterol-rich domains, we assessed the co-localization of the GFP-tagged receptors with that of cholera toxin B-Alexa Fluor 555. We performed quantitative co-localization between transfected receptors and cholera toxin within the plasma membrane, by measuring two different parameters: Pearson's correlation coefficient and intensity correlation quotient (Manders *et al.*, 1993; Li *et al.*, 2004). This analysis demonstrated that the plasma membrane-associated pool of the wild-type receptor was strongly associated with lipid rafts (Figure 3 and Table 1). On the contrary, little co-localization was seen between CB_1(C415A)-GFP receptor and cholera toxin B, indicating that the mutant receptor markedly lost its association with lipid rafts on the plasma membrane (Figure 6C, and Table 1). Also in this case, we found that the co-localization parameters of the two receptors with cholera toxin B were independent of their expression level (data not shown), ruling out the possibility that the different lipid rafts

Table 1

Surface expression, raft association, and functional parameters of CB_1-GFP and CB_1(C415A)-GFP receptors in SH-SY5Y cells

Receptor	Overlap coefficient with DiC_{16} (-TX100)	DRM remnant (%)	Overlap coefficient with $DiIC_{16}$ (+TX100)	Pearson's correlation coefficient with CTB	Intensity correlation quotient with CTB	Diffusion coefficient ($\mu m^2 \cdot s^{-1}$)	Immobile fraction (%)
CB_1-GFP	0.75 ± 0.04	20 ± 5	0.70 ± 0.05	0.74 ± 0.04	0.21 ± 0.03	0.46 ± 0.05	12 ± 6
CB_1(C415A)-GFP	0.52 ± 0.05*	15 ± 5	0.18 ± 0.01***	0.27 ± 0.04***	0.05 ± 0.01***	0.63 ± 0.06*	7 ± 4

TX100, Triton X-100. CTB, cholera toxin B. Data are mean ± SEM. See text for details. *$P < 0.05$ versus CB_1-GFP receptor; ***$P < 0.001$ versus CB_1-GFP receptor.

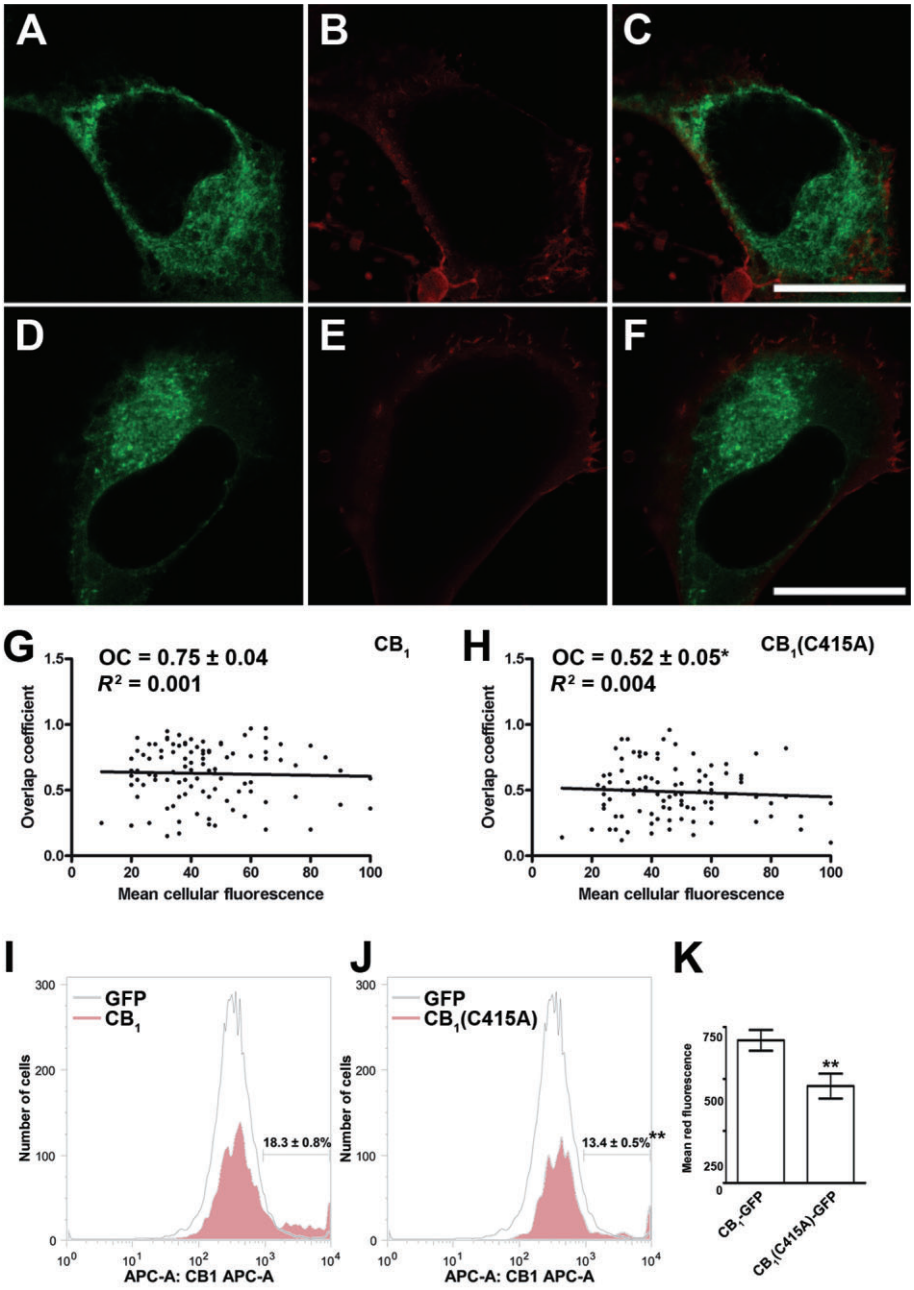

Figure 5

Membrane targeting of CB_1-GFP and CB_1(C415A)-GFP receptors. Details are given under Methods, and numerical values are summarized in Table 1. (A–F) Double staining of SH-SY5Y cells expressing CB_1-GFP (A) and CB_1(C415A)-GFP (D) receptors together with $DiIC_{16}$ (B and E) for plasma membrane staining. Merged images are shown in the panels C and F. Scale bars, 10 μm. Images are representative of three independent experiments, for a total of 18–27 cells. (G and H) Graphs showing the overlap coefficient (i.e. the degree of overlap between $DiIC_{16}$ and GFP-tagged receptors fluorescence, as described under Methods) versus the mean green fluorescence intensity (i.e. a measure of CB_1-GFP [G] and CB_1[C415A]-GFP [H] expression in each cell) for 100 transfected cells. The overlap coefficient and the expression level were not correlated for either receptor ($R^2 < 0.005$). (I and J) Detection of surface expression of CB_1 receptors by FACS. GFP-transfected cells and cells overexpressing wild-type (G) and mutant (H) CB_1 receptors were incubated with anti-CB_1 PA1-745, and were analysed by indirect immunofluorescence using allophycocyanin-labelled secondary antibody. The red fluorescence analysis was performed only on the GFP-positive fraction. The displayed patterns are representative of three independent experiments. (K) Mean red fluorescence obtained for the wild-type and mutant CB_1 receptors. The mean red fluorescence was calculated within the gates shown in panels G and H. A typical experiment out of the three performed independently is represented. $^{**}P < 0.01$ versus CB_1-GFP receptor.

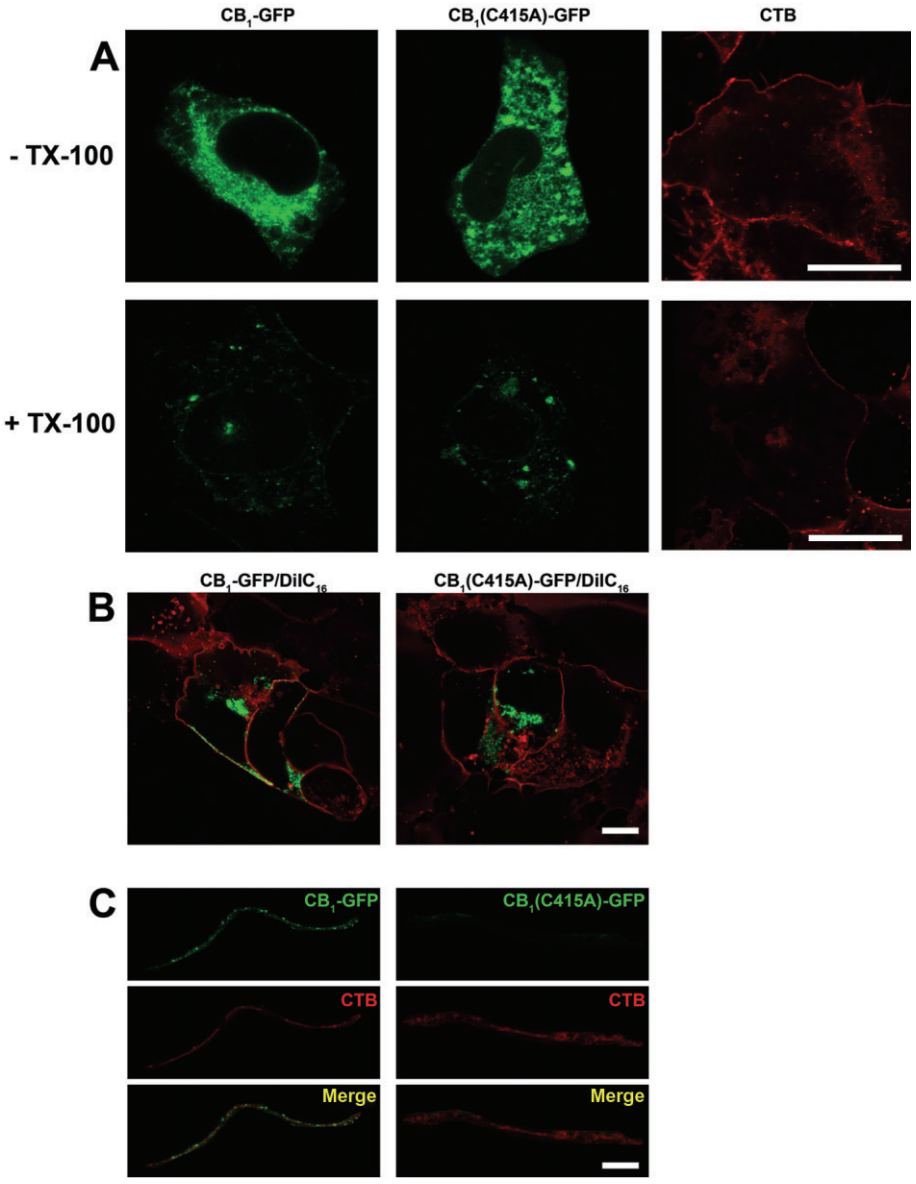

Figure 6

Confocal microscopy analysis of raft targeting of CB_1-GFP and CB_1(C415A)-GFP receptors in SH-SY5Y cells. Details are as given under Methods and numerical values are summarized in Table 1. Images are representative of three independent experiments for a total of 18–27 cells. (A) Triton X-100 (TX-100) extraction assay. CB_1-GFP and CB_1(C415A)-GFP transfected cells were imaged before (top panels) and after (bottom panels) detergent incubation. Scale bars, 10 μm. (B) Triton X-100 extracted cells expressing both receptors were double-stained with $DiIC_{16}$. Scale bars, 10 μm. (C) Co-localization analysis of the distribution of CB receptors and cholera toxin B (CTB) in Triton X-100 extracted cells. Merged images are shown in the bottom panels. Scale bars, 2 μm.

distribution of wild-type and mutant CB_1 receptors may be due to a different receptor expression within single observed cells.

Diffusional properties of CB_1 and CB_1(C415A) receptors in membranes under steady-state conditions

We used confocal FRAP to compare the diffusional mobility of wild-type and C415A mutant receptors expressed in SH-SY5Y cells under basal conditions (Figure 7 and Table 1). This analysis revealed that the diffusion coefficient of the C415A mutant receptor was ~1.3-fold higher than that of wild-type ($P < 0.05$, Table 1). No significant difference was observed between the immobile fraction of the two GFP-tagged receptors (Table 1).

Cys^{415} is not involved in agonist binding affinity, but is essential for G-protein coupling of CB_1 receptors and for subsequent inhibition of adenylyl cyclase

The binding parameters (K_d and B_{max}) of wild-type and C415A CB_1 receptors were determined in HEK-293 cells through

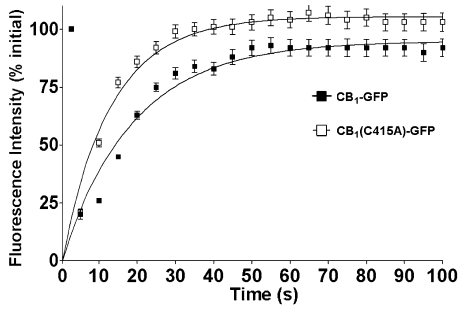

Figure 7

Diffusional mobility of CB_1-GFP and CB_1(C415A)-GFP receptors in the plasma membrane measured by confocal FRAP. Details are given under Methods and derived values are summarized in Table 1. Recovery curves from plasma-associated pools of CB_1-GFP and CB_1(C415A)-GFP receptors transiently transfected in SH-SY5Y. Data show the mean ± S.E.M for 9 cells and are from a representative experiment (out of three independent experiments).

competition binding assays, using [^{3}H]CP55940 as radioligand (Figure 8A, Table 2). The wild-type and C415A receptors yielded similar binding curves with similar K_d values, suggesting that the mutant receptor retained the proper folding and gross structural features of the wild-type CB_1 receptor. However, the B_{max} value for the C415A receptor was ~70% of the B_{max} value for the wild-type , indicating that cells expressing the mutant receptor have substantially fewer functional receptors with wild-type-like binding affinity compared with cells expressing the native receptor. These data are in agreement with the results of both confocal and FACS analyses, that showed a similar reduction in the expression of the mutant receptor at the plasma membrane level, compared with the wild-type.

To assess the effect of the C415A mutation on the functional properties of CB_1 receptors, the ability of CP55940 to stimulate the binding of [^{35}S]GTPγS was measured (Figure 8B, Table 2). The EC_{50} value of the wild-type receptor for the CP55940 agonist was 54 ± 2 nM, whereas the C415A mutant showed virtually no [^{35}S]GTPγS binding under the same

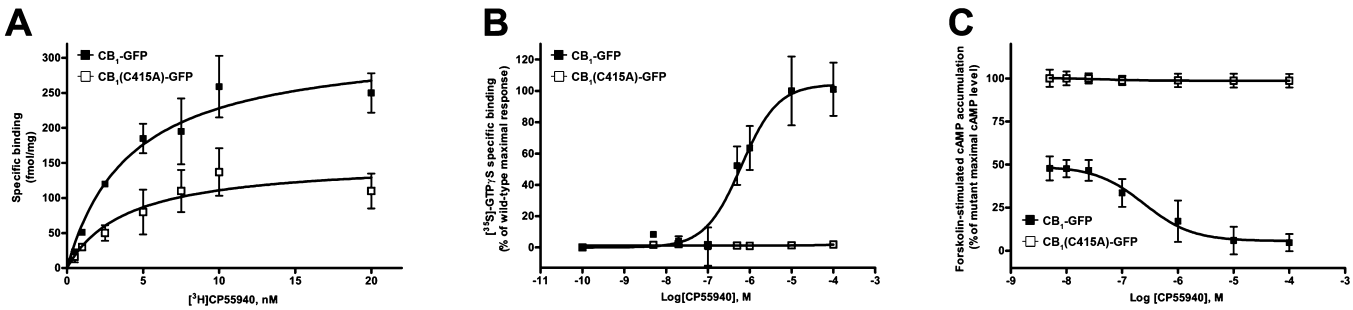

Figure 8

Function of CB_1-GFP and CB_1(C415A)-GFP receptors in HEK-293 cells**.** CB_1-GFP or CB_1(C415)-GFP were transiently transfected into HEK-293 cells and their function was tested. Details are given under Methods, and numerical values are summarized in Table 2. (A) Saturation binding curves for the CB_1 receptor agonist [^{3}H]CP55940 on plasma membrane preparations from cells expressing CB_1-GFP and CB_1(C415)-GFP receptors. Membranes were incubated with different concentrations of [^{3}H]CP55940 at 37°C for 60 min. (B) Stimulation of [^{35}S]GTPγS binding by CP55940 in whole cells expressing CB_1-GFP and CB_1(C415A)-GFP receptors. Values are mean (±SEM) percentage of maximal wild-type stimulation (18000 ± 3000 cpm), from at least three independent experiments, each performed in triplicate. (C) Dose-dependence of cAMP biosynthesis in cells over-expressing the CB_1-GFP and CB_1(C415A)-GFP receptors. Cells were incubated with 0.45 μM forskolin and varying concentrations of CP55940, as described in Methods. Values are mean (±SEM) percentage of maximal level of cAMP in cells with mutant receptors (3.8 ± 0.2 pmol per 10^4 cells), from at least three independent experiments, each performed in triplicate.

Table 2

Affinity and activity data for the CB_1-GFP and CB_1(C415A)-GFP receptors in HEK-293 cells. See text for details

Receptor	CP55940 binding K_d (nM)	CP55940 binding B_{max} (fmol·mg^{-1})	GTPγS EC_{50} (nM)	GTPγS Emax (% of wild-type)	cAMP EC_{50} (nM)	cAMP Max count (% of wild-type)
CB_1-GFP	4.2 ± 0.6	174 ± 8	54 ± 2	109 ± 10	420 ± 75	98 ± 4
CB_1(C415A)-GFP	3.9 ± 0.3	116 ± 12***	ND	ND	ND	2.8 ± 0.3***

Data are mean ± SEM. See text for details. ***P < 0.001 versus CB_1-GFP receptor.
ND, not detectable.

Table 3

Agonist independent signalling of CB_1-GFP and CB_1(C415A)-GFP in SH-SY5Y cells and HEK-293 cells

Cell line	GTPγS binding (fold of stimulation over GFP-transfected cells)		cAMP level (fold of inhibition over GFP-transfected cells)	
	CB_1-GFP	CB_1(C415A)-GFP	CB_1-GFP	CB_1(C415A)-GFP
SH-SY5Y	17 ± 6[a]	3 ± 1***	2.9 ± 1.1[c]	1.4 ± 0.3*
HEK-293	29 ± 8[b]	4 ± 1***	2.1 ± 1.2[d]	1.1 ± 0.2*

Data are means ± SEM values; $n = 6$ for each value. ***$P < 0.001$ versus CB_1-GFP receptor. *$P < 0.05$ versus CB_1-GFP receptor.
[a]GFP-transfected cells = 340 ± 30 cpm. [b]GFP-transfected cells = 430 ± 50 cpm. [c]GFP-transfected cells = 1.3 ± 0.1 pmol per 10^4 cells.
[d]GFP-transfected cells = 4.2 ± 0.2 pmol per 10^4 cells.

conditions; this observation indicates that Cys^{415} is a critical residue for the functional coupling of the CB_1 receptor to its G-proteins. This concept was further supported by evaluating the ability of wild-type and mutant receptors to inhibit adenylyl cyclase. cAMP production, stimulated by forskolin was inhibited by increasing concentrations of CP55940 in cells that overexpressed CB_1-GFP, but not in those that overexpressed CB_1(C415)-GFP receptors (Figure 8C, Table 2).

In the absence of CP55940, the basal constitutive [^{35}S]GTPγS binding activity of the mutant CB_1 was approximately sevenfold lower compared with that of the of wild-type receptor (1714 cpm vs. 12 388 cpm; $P < 0.001$). Additionally, compared with cells transfected with the wild-type receptor, those transiently expressing the mutant receptor showed a 50% reduction ($P < 0.05$) of their efficacy in reducing cAMP accumulation upon forskolin stimulation, further suggesting that the C415A substitution affected the basal constitutive capacity of CB_1 receptors to inhibit adenylyl cyclase. Remarkably, similar results were obtained in SH-SY5Y cells (Table 3).

Palmitoylation is a determinant in the coupling of CB_1 receptor with $G\alpha_{i3}$ and $G\alpha_o$, but not to $G\alpha_{i2}$ proteins

Finally, we tested whether the observed impairment in CB_1(C415A) receptor signalling was due to a reduction in coupling to specific subsets of $G\alpha_{i/o}$ proteins. To this end, we determined whether palmitoylation/depalmitoylation state of CB_1 receptors as well as of its associated G-proteins could influence their interactions. Thus, rat forebrain or N18TG2 cell membranes were either depalmitoylated with hydroxylamine to break thioesters, or were left untreated (controls). Treated and control membranes were washed and then re-palmitoylated with palmitoyl-CoA. Hydroxylamine treatment led to the disruption of CB_1-$G\alpha_{i3}$ or $G\alpha_o$ coupling, but not to that of CB_1-$G\alpha_{i2}$ (Figure 6), nor of CB_1-$G\alpha_{i1}$ (data not shown). These findings indicate that palmitoylation is a determinant in the specific coupling of CB_1 receptors with $G\alpha_{i3}$ and $G\alpha_o$, two G-proteins known to interact with the helix 8 of the receptor; however, it did not affect coupling to $G\alpha_{i2}$, which interacts with the third intracellular loop of the receptor (Figure 1). It is noteworthy that no further increase in the CB_1-$G\alpha_i$ coupling was observed when non-depalmitoylated membrane proteins were subjected to palmitoylation, and that re-palmitoylation of depalmitoylated CB_1 receptors failed to restore their association with $G\alpha_{i3}$ or $G\alpha_o$.

Discussion

Almost all members of the class A rhodopsin-like family of GPCRs are post-translationally modified with one or more palmitic acid(s) covalently bound to cysteine(s) located at the end of the juxtamembrane C-terminal segment (or helix 8, Figure 1), a modification that is critical for receptor localization and/or activity (Chini and Parenti, 2009). The results presented here demonstrated that CB_1 receptors were post-translationally modified by palmitoylation at Cys^{415}, and that substitution of this residue yielded a receptor with impaired membrane targeting and signalling.

In vivo studies demonstrated that the CB_1 receptor is palmitoylated in rat forebrain neurones, and that this covalent modification is required for its efficient coupling with a specific subset of G-proteins, namely $G\alpha_{i3}$ or $G\alpha_o$, but not $G\alpha_{i2}$ proteins. One possible interpretation of these findings is that the treatment that removes the palmitoyl tail from the CB_1 receptor might disrupt its ability to remain anchored in the membrane subdomains along with its assigned G-proteins. However, because GPCR-associated $G\alpha_{i/o}$ proteins are also palmitoylated (Duncan and Gilman, 1996; Loisel *et al.*, 1996), it is also possible that the hydroxylamine treatment would depalmitoylate $G\alpha_{i3}$ or $G\alpha_o$, thereby affecting their association with CB_1 receptors. In line with this, the palmitoylation state of proteins has been associated with their compartmentalization within lipid rafts, where a physical interaction with specific raft-enriched G-proteins may take place (Greaves and Chamberlain, 2007; Greaves *et al.*, 2009). The translocation of these complexes in and out of membrane compartments such as lipid rafts may be integral to the signalling process (see Vogler *et al.*, 2008). For instance, experimental evidence supports a selective coupling of β_2-adrenoceptors to $G\alpha_i$ proteins within lipid rafts, whereas β_1-adrenoceptor coupling to $G\alpha_s$ occurs outside these compartments (Rybin *et al.*, 2000; Xiang *et al.*, 2002). Also GTP-$G\alpha_i$ and its signalling effector adenylyl cyclase (type 5/6) co-localized to lipid raft-like compartments (Huang *et al.*, 1997; Rybin *et al.*, 2000), suggesting a role for these membrane microdomains in their signal transduction pathway. To complete the G-protein cycle, the interaction of $G\alpha_i$ with $G\beta\gamma$, that occurs outside lipid rafts

(Moffett *et al.*, 2000), may facilitate the re-establishment of a CB_1-G-protein heterotrimer complex (Vogler *et al.*, 2008). Thus, failure of $G\alpha_{i3}$ and $G\alpha_o$ proteins to interact with CB_1 receptors after depalmitoylation may reflect the disruption of the translocation of critical protein components, perhaps as the result of faulty repalmitoylation.

To further investigate the role of palmitoylation on CB_1 receptor function, we performed *in vitro* studies using GFP-tagged wild-type (CB_1-GFP) and mutant (CB_1[C415A]-GFP) proteins. In the latter, Cys^{415}, the only potential palmitoylation site present in the helix 8, was substituted with an alanine, a residue that cannot be covalently modified. Our findings demonstrated that Cys^{415}, by serving as the palmitoylation site in CB_1 receptors, has a key role in regulating CB_1 receptor localization and functioning.

Flow cytometry and binding studies demonstrated that CB_1(C415A)-GFP was significantly less efficiently targeted into the plasma membrane than CB_1-GFP. Western blotting and flow cytometry demonstrated that wild-type and C415A receptors exhibited similar levels of expression within the cells, suggesting that the reduction in the cell surface accumulation was not due to a reduced synthesis. Unexpectedly, there was no correlation between total expression levels of CB_1 receptors and plasma membrane expression. We interpret these results as showing that, because the CB_1 receptors are constitutively localized intracellularly (Sarnataro *et al.*, 2005; Rozenfeld and Devi, 2008), additional specific factors may be required for the receptors to be enriched in the plasma membrane. As for other GPCRs like thyrotropin (Tanaka *et al.*, 1998), δ-opioid (Petaja-Repo *et al.*, 2006) and dopamine D_1 (Ng *et al.*, 1994) receptors, the lack of palmitoylation appears to reduce the steady-state level of the protein on the plasma membrane. It has been suggested that a cycle of palmitoylation/depalmitoylation could regulate receptor progression along the biosynthetic route from synthesis to plasma membrane localization (Chini and Parenti, 2009); however, the molecular mechanisms involved in this process are not yet disclosed. Our results suggest that Cys^{415}, possibly via its reversible palmitoylation, is a critical residue in controlling the plasma membrane targeting of CB_1 receptors.

The lateral mobility of a GPCR on the plasma membrane is a prerequisite for interactions with G-proteins, and has a significant impact on the overall efficiency of its signal transduction. We used FRAP to compare, in living cells, the cell surface dynamics of CB_1-GFP and CB_1(C415A)-GFP receptors within the plasma membrane. The two receptors displayed similar immobile fractions, but different diffusion coefficients, with the wild-type diffusing more slowly than the mutant. These data suggest that a small subset (~10%) of both receptors was immobile, a finding that could be attributed to stable interaction of these receptors with the peripheral cytoskeleton or with the extracellular matrix. The increase in the diffusion coefficient calculated for the CB_1(C415A)-GFP receptor can be interpreted as a result of a less stable interaction of the mutant protein with large or fixed molecules. Alternatively, the observed change in the receptor membrane dynamics could be explained by the possibility that the two receptors reside preferentially into distinct membrane microenvironments with different viscosity, such as raft and non-raft domains (Dainese *et al.*, 2007; 2010). In the latter case, anchoring provided by the palmitoylation cannot reduce *per se* receptor mobility; however, it might allow complex formation with other factors that restrict diffusion of CB_1 receptors, as observed for other palmitoylated proteins (Miura *et al.*, 2006). Thus, palmitoylation of CB_1-GFP seems to increase the interaction with more packed and stable lipids belonging to subdomains of the membrane (Melkonian *et al.*, 1999), such as lipid rafts, where lateral diffusion is reduced (Dainese *et al.*, 2010). Finally, by analogy with the recently resolved X-ray structure of the β_2-adrenoceptor where more stable homodimers interact through palmitate residues bridged by two cholesterol molecules (Cherezov *et al.*, 2007), palmitoylation of CB_1 receptors may also play an important role in forming more stable forms of the receptor.

As mentioned before, the palmitoylation state of proteins has been associated with movements in and out of rigid lipid raft compartments of the plasma membrane (Greaves and Chamberlain, 2007). We have previously demonstrated that ~20% of the wild-type CB_1 receptor was confined to the DRMs (Oddi *et al.*, 2011). Here, we confirmed the raft association of CB_1 receptors also by quantitative co-localization with cholera toxin B, a specific marker of the lipid raft constituent ganglioside GM_1. Compared with the wild-type receptor, the C415A mutant seems to have a lower propensity to co-localize within lipid rafts, suggesting a functional involvement of C415 palmitoylation in DRM targeting of CB_1 receptors. A similar mechanism has also been shown for membrane-targeting of 5-HT_{1A} receptors (Renner *et al.*, 2007). In this context, it has been proposed that the 16-carbon saturated chain of palmitic acid is well-packed within the liquid-ordered phase of lipid rafts, increasing the affinity of the protein for such sphingolipid/cholesterol-enriched domains (Melkonian *et al.*, 1999). However, a general role of palmitoylation as a raft targeting signal for integral membrane proteins is still controversial (van Duyl *et al.*, 2002).

The finding that the C415A mutant displayed virtually no [^{35}S]GTPγS binding upon agonist treatment indicates that Cys^{415} played an essential role also in the functional coupling of this receptor to its specific subset of $G_{i/o}$ proteins. This conclusion was further supported by the lack of adenylyl cyclase inhibition upon agonist binding to mutant receptors. Moreover, the C415A mutation strongly affected the basal (agonist-independent) activity of CB_1 receptors, as shown by the lower constitutive activity exhibited by the mutant in [^{35}S]GTPγS and cAMP assays. These findings can only be partly explained by the reduced amount of CB_1 mutant receptors on the plasma membrane, as well as within the lipid rafts (Figure 2 and Table 1). The almost complete absence of functional activity of C415A receptor in these assays indicates that, besides regulating receptor trafficking, Cys^{415} may also impact on the ability of CB_1 receptors to physically interact with its specific subset of G-proteins. From this point of view, Cys^{415} may play a structural role as the residue that anchors the proximal portion of the carboxyl tail of CB_1 receptors to the lipid bilayer. This fact would create the fourth intracellular loop (corresponding to helix 8 in Figure 1), that might be critical for the formation of a G-protein binding site, as already reported in the X-ray crystal structures of both rhodopsin and β_2-adrenoceptors (Palczewski *et al.*, 2000; Cherezov *et al.*, 2007; Rosenbaum *et al.*, 2007). This view is substantiated by our *in vivo* results, showing that the depalmitoylated CB_1 receptor loses the ability to bind G-proteins

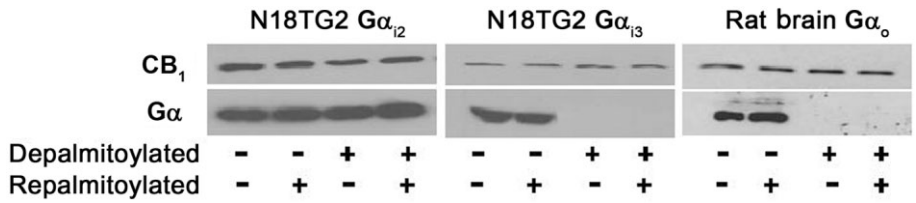

Figure 9

Effect of depalmitoylation on CB_1 receptor association with Gα proteins in N18TG2 cells or in rat forebrain membranes. Details are given under Methods. After each treatment, P2 membrane fractions were immunoprecipitated with CB_1 receptor antibodies, and Western blots were performed after SDS-urea-10% PAGE, with detection by N-terminal CB_1 receptor antibody and anti-$G\alpha_{i2}$, $G\alpha_{i3}$ or $G\alpha_o$ specific antibodies, as indicated. Blots are representative of three independent experiments.

(Figure 9). In further support of this hypothesis, previous studies reported that the helix 8 of CB_1 receptors binds and directly activates several subtypes of $G\alpha_{i/o}$ proteins (Mukhopadhyay and Howlett, 2001). More recently, Ahn and colleagues have demonstrated that the formation and stability of helix 8 in CB_1 receptors is important for receptor localization and, consequently, for its functional coupling with G-proteins (Ahn *et al.*, 2010). Finally, it is noteworthy that a similar role for Cys^{313} and Cys^{320} (Figure 1) in coupling CB_2 receptors to adenylyl cyclase has been previously established (Feng and Song, 2001), highlighting the functional importance of conserved cysteines in the C-terminal juxtamembrane region of cannabinoid receptors. However, the functional relevance of helix 8 cannot be extended to all GPCR members, because the recently solved crystal structure of the CXCR4 chemokine receptor does not show the presence of an helix 8, although its C-terminus contains a 'palmitoylable' cysteine residue (Wu *et al.*, 2010).

In conclusion, we have demonstrated that, besides the cholesterol-binding CRAC motif (Oddi *et al.*, 2011), another lipid-interacting residue might direct the interaction of CB_1 receptors with the surrounding membrane lipids, that is Cys^{415} in its C-terminal domain. The data presented here suggest that palmitoylation of this residue may be used by cells to direct CB_1 receptor targeting to cholesterol-rich subdomains of the plasma membrane, thus influencing, directly or indirectly, its interaction with some G-proteins. On a final note, the sensitivity of the CB_1 receptor to membrane lipids supports the concept of a new paradigm of ligand-receptor interaction, whereby a third player comes into the game: the membrane lipids (Maccarrone, 2008). As a consequence, the membrane environment might play a role in endocannabinoid signalling, with a potential impact on different neurotransmission pathways, as well as on neurodegenerative/neuroinflammatory diseases, where the CB_1 receptor is known to be involved.

Acknowledgements

The authors thank Dr Lucilla Bongiorno (University of Rome 'Tor Vergata') for her technical support in plasmid preparation. Financial support from Ministero dell'Istruzione, dell'Università e della Ricerca (PRIN 2008 grant), and from Fondazione TERCAS (grant 2009–2012) to M.M. is gratefully acknowledged. A.C.H., S.M and S.S. were supported by National Institute on Drug Abuse (USA) grants R01-DA03690, K05-DA00182 and U24-12385).

Conflicts of interest

None.

References

Ahn KH, Nishiyama A, Mierke DF, Kendall DA (2010). Hydrophobic residues in helix 8 of cannabinoid receptor 1 are critical for structural and functional properties. Biochemistry 49: 502–511.

Alexander SPH, Mathie A, Peters JA (2011). Guide to Receptors and Channels (GRAC), 5th Edition. Br J Pharmacol 164 (Suppl. 1): S1–S324.

Anderson RG, Jacobson K (2002). A role for lipid shells in targetinG-proteins to caveolae, rafts, and other lipid domains. Science 296: 1821–1825.

Bari M, Battista N, Fezza F, Finazzi-Agrò A, Maccarrone M (2005). Lipid rafts control signaling of type-1 cannabinoid receptors in neuronal cells. Implications for anandamide-induced apoptosis. J Biol Chem 280: 12212–12220.

Bari M, Oddi S, De Simone C, Spagnolo P, Gasperi V, Battista N *et al.* (2008). Type-1 cannabinoid receptors colocalize with caveolin-1 in neuronal cells. Neuropharmacology 54: 45–50.

Beck M, Brickley K, Wilkinson HL, Sharma S, Smith M, Chazot PL *et al.* (2002). Identification, molecular cloning, and characterization of a novel $GABA_A$ receptor-associated protein, GRIF-1. J Biol Chem 277: 30079–30090.

Bolte S, Cordelieres FP (2006). A guided tour into subcellular colocalization analysis in light microscopy. J Microsc 224: 213–232.

Bouaboula M, Perrachon S, Milligan L, Canat X, Rinaldi-Carmona M, Portier M *et al.* (1997). A selective inverse agonist for central cannabinoid receptor inhibits mitogen-activated protein kinase activation stimulated by insulin or insulin-like growth factor 1. Evidence for a new model of receptor/ligand interactions. J Biol Chem 272: 22330–22339.

Centonze D, Finazzi-Agrò A, Bernardi G, Maccarrone M (2007). The endocannabinoid system in targeting inflammatory neurodegenerative diseases. Trends Pharmacol Sci 28: 180–187.

Chen C, Shahabi V, Xu W, Liu-Chen LY (1998). Palmitoylation of the rat mu opioid receptor. FEBS Lett 441: 148–152.

Cherezov V, Rosenbaum DM, Hanson MA, Rasmussen SG, Thian FS, Kobilka TS *et al.* (2007). High-resolution crystal structure of an engineered human beta2-adrenergic G-protein-coupled receptor. Science 318: 1258–1265.

Chini B, Parenti M (2009). G-protein-coupled receptors, cholesterol and palmitoylation: facts about fats. J Mol Endocrinol 42: 371–379.

Cravatt BF, Lichtman AH (2004). The endogenous cannabinoid system and its role in nociceptive behavior. J Neurobiol 61: 149–160.

Cravatt BF, Demarest K, Patricelli MP, Bracey MH, Giang DK, Martin BR *et al.* (2001). Supersensitivity to anandamide and enhanced endogenous cannabinoid signaling in mice lacking fatty acid amide hydrolase. Proc Natl Acad Sci U S A 98: 9371–9376.

Dainese E, Oddi S, Bari M, Maccarrone M (2007). Modulation of the endocannabinoid system by lipid rafts. Curr Med Chem 14: 2702–2715.

Dainese E, Oddi S, Maccarrone M (2010). Interaction of endocannabinoid receptors with biological membranes. Curr Med Chem 17: 1487–1499.

Di Marzo V (2008). Targeting the endocannabinoid system: to enhance or reduce? Nat Rev Drug Discov 7: 438–455.

Drisdel RC, Manzana E, Green WN (2004). The role of palmitoylation in functional expression of nicotinic alpha7 receptors. J Neurosci 24: 10502–10510.

Drisdel RC, Alexander JK, Sayeed A, Green WN (2006). Assays of protein palmitoylation. Methods 40: 127–134.

Duncan JA, Gilman AG (1996). Autoacylation of G-protein alpha subunits. J Biol Chem 271: 23594–23600.

Duncan M, Davison JS, Sharkey KA (2005). Review article: endocannabinoids and their receptors in the enteric nervous system. Aliment Pharmacol Ther 22: 667–683.

van Duyl BY, Rijkers DT, de Kruijff B, Killian JA (2002). Influence of hydrophobic mismatch and palmitoylation on the association of transmembrane alpha-helical peptides with detergent-resistant membranes. FEBS Lett 523: 79–84.

Eroglu C, Brugger B, Wieland F, Sinning I (2003). Glutamate-binding affinity of Drosophila metabotropic glutamate receptor is modulated by association with lipid rafts. Proc Natl Acad Sci U S A 100: 10219–10224.

Fay JF, Dunham TD, Farrens DL (2005). Cysteine residues in the human cannabinoid receptor: only C257 and C264 are required for a functional receptor, and steric bulk at C386 impairs antagonist SR141716A binding. Biochemistry 44: 8757–8769.

Feng W, Song ZH (2001). Functional roles of the tyrosine within the NP(X)(n)Y motif and the cysteines in the C-terminal juxtamembrane region of the CB2 cannabinoid receptor. FEBS Lett 501: 166–170.

Fukushima Y, Saitoh T, Anai M, Ogihara T, Inukai K, Funaki M *et al.* (2001). Palmitoylation of the canine histamine H2 receptor occurs at Cys(305) and is important for cell surface targeting. Biochim Biophys Acta 1539: 181–191.

Gimpl G, Burger K, Fahrenholz F (1997). Cholesterol as modulator of receptor function. Biochemistry 36: 10959–10974.

Greaves J, Chamberlain LH (2007). Palmitoylation-dependent protein sorting. J Cell Biol 176: 249–254.

Greaves J, Prescott GR, Gorleku OA, Chamberlain LH (2009). The fat controller: roles of palmitoylation in intracellular protein trafficking and targeting to membrane microdomains (Review). Mol Membr Biol 26: 67–79.

Guzzi F, Zanchetta D, Cassoni P, Guzzi V, Francolini M, Parenti M *et al.* (2002). Localization of the human oxytocin receptor in caveolin-1 enriched domains turns the receptor-mediated inhibition of cell growth into a proliferative response. Oncogene 21: 1658–1667.

Hagmann J, Fishman PH (1982). Detergent extraction of cholera toxin and gangliosides from cultured cells and isolated membranes. Biochim Biophys Acta 720: 181–187.

Harvey MJ, Giupponi G, De Fabritiis G (2009). ACEMD: accelerating biomolecular dynamics in the microsecond time scale. J Chem Theory Comput 5: 1632–1639.

Houston DB, Howlett AC (1993). Solubilization of the cannabinoid receptor from rat brain and its functional interaction with guanine nucleotide-bindinG-proteins. Mol Pharmacol 43: 17–22.

Howlett AC (2005). A short guide to the nomenclature of seven-transmembrane spanning receptors for lipid mediators. Life Sci 77: 1522–1530.

Howlett AC, Song C, Berglund BA, Wilken GH, Pigg JJ (1998). Characterization of CB1 cannabinoid receptors using receptor peptide fragments and site-directed antibodies. Mol Pharmacol 53: 504–510.

Huang C, Hepler JR, Chen LT, Gilman AG, Anderson RG, Mumby SM (1997). Organization of G-proteins and adenylyl cyclase at the plasma membrane. Mol Biol Cell 8: 2365–2378.

Jing SQ, Trowbridge IS (1990). Nonacylated human transferrin receptors are rapidly internalized and mediate iron uptake. J Biol Chem 265: 11555–11559.

Kalipatnapu S, Chattopadhyay A (2004). A GFP fluorescence-based approach to determine detergent insolubility of the human serotonin1A receptor. FEBS Lett 576: 455–460.

Karnik SS, Ridge KD, Bhattacharya S, Khorana HG (1993). Palmitoylation of bovine opsin and its cysteine mutants in COS cells. Proc Natl Acad Sci U S A 90: 40–44.

Kathuria S, Gaetani S, Fegley D, Valino F, Duranti A, Tontini A *et al.* (2003). Modulation of anxiety through blockade of anandamide hydrolysis. Nat Med 9: 76–81.

Klein TW (2005). Cannabinoid-based drugs as anti-inflammatory therapeutics. Nat Rev Immunol 5: 400–411.

Leterrier C, Bonnard D, Carrel D, Rossier J, Lenkei Z (2004). Constitutive endocytic cycle of the CB1 cannabinoid receptor. J Biol Chem 279: 36013–36021.

Li Q, Lau A, Morris TJ, Guo L, Fordyce CB, Stanley EF (2004). A syntaxin 1, Galpha(o), and N-type calcium channel complex at a presynaptic nerve terminal: analysis by quantitative immunocolocalization. J Neurosci 24: 4070–4081.

Linder ME, Middleton P, Hepler JR, Taussig R, Gilman AG, Mumby SM (1993). Lipid modifications of G-proteins: alpha subunits are palmitoylated. Proc Natl Acad Sci U S A 90: 3675–3679.

Loisel TP, Adam L, Hebert TE, Bouvier M (1996). Agonist stimulation increases the turnover rate of beta 2AR-bound palmitate and promotes receptor depalmitoylation. Biochemistry 35: 15923–15932.

Maccarrone M (2006). *The Brain and the Body's Marijuana and Beyond*. CRC Press: Boca Raton, FL. pp. 451–466.

Maccarrone M (2008). Good news for CB1 receptors: endogenous agonists are in the right place. Br J Pharmacol 153: 179–181.

Maccarrone M, Battista N, Centonze D (2007). The endocannabinoid pathway in Huntington's disease: a comparison with other neurodegenerative diseases. Prog Neurobiol 81: 349–379.

Maccarrone M, Gasperi V, Catani MV, Diep TA, Dainese E, Hansen HS *et al.* (2010). The endocannabinoid system and its relevance for nutrition. Annu Rev Nutr 30: 423–440.

Manders EMM, Verbeek FJ, Aten JA (1993). Measurement of co-localization of objects in dual-colour confocal images. J Microsc 169: 375–382.

Marchant JS, Subramanian VS, Parker I, Said HM (2002). Intracellular trafficking and membrane targeting mechanisms of the human reduced folate carrier in Mammalian epithelial cells. J Biol Chem 277: 33325–33333.

Melkonian KA, Ostermeyer AG, Chen JZ, Roth MG, Brown DA (1999). Role of lipid modifications in targetinG-proteins to detergent-resistant membrane rafts. Many raft proteins are acylated, while few are prenylated. J Biol Chem 274: 3910–3917.

Milligan G, Grassie MA, Wise A, MacEwan DJ, Magee AI, Parenti M (1995). G-protein palmitoylation: regulation and functional significance. Biochem Soc Trans 23: 583–587.

Miura GI, Buglino J, Alvarado D, Lemmon MA, Resh MD, Treisman JE (2006). Palmitoylation of the EGFR ligand Spitz by Rasp increases Spitz activity by restricting its diffusion. Dev Cell 10: 167–176.

Moffett S, Brown DA, Linder ME (2000). Lipid-dependent targeting of G-proteins into rafts. J Biol Chem 275: 2191–2198.

Mukhopadhyay S, Howlett AC (2001). CB1 receptor-G-protein association. Subtype selectivity is determined by distinct intracellular domains. Eur J Biochem 268: 499–505.

Mukhopadhyay S, Howlett AC (2005). Chemically distinct ligands promote differential CB1 cannabinoid receptor-Gi protein interactions. Mol Pharmacol 67: 2016–2024.

Navratil AM, Bliss SP, Berghorn KA, Haughian JM, Farmerie TA, Graham JK *et al.* (2003). Constitutive localization of the gonadotropin-releasing hormone (GnRH) receptor to low density membrane microdomains is necessary for GnRH signaling to ERK. J Biol Chem 278: 31593–31602.

Ng GY, Mouillac B, George SR, Caron M, Dennis M, Bouvier M *et al.* (1994). Desensitization, phosphorylation and palmitoylation of the human dopamine D1 receptor. Eur J Pharmacol 267: 7–19.

Nichols BJ, Kenworthy AK, Polishchuk RS, Lodge R, Roberts TH, Hirschberg K *et al.* (2001). Rapid cycling of lipid raft markers between the cell surface and Golgi complex. J Cell Biol 153: 529–541.

Oddi S, Dainese E, Fezza F, Lanuti M, Barcaroli D, De Laurenzi V *et al.* (2011). Functional characterization of putative cholesterol binding sequence (CRAC) in human type-1 cannabinoid receptor. J Neurochem 116: 858–865.

Okamoto T, Schlegel A, Scherer PE, Lisanti MP (1998). Caveolins, a family of scaffoldinG-proteins for organizing 'preassembled signaling complexes' at the plasma membrane. J Biol Chem 273: 5419–5422.

Paila YD, Ganguly S, Chattopadhyay A (2010). Metabolic depletion of sphingolipids impairs ligand binding and signaling of human serotonin1A receptors. Biochemistry 49: 2389–2397.

Palczewski K, Kumasaka T, Hori T, Behnke CA, Motoshima H, Fox BA *et al.* (2000). Crystal structure of rhodopsin: a G-protein-coupled receptor. Science 289: 739–745.

Pertwee RG (2005). Pharmacological actions of cannabinoids. Handb Exp Pharmacol 168: 1–51.

Petaja-Repo UE, Hogue M, Leskela TT, Markkanen PM, Tuusa JT, Bouvier M (2006). Distinct subcellular localization for constitutive and agonist-modulated palmitoylation of the human delta opioid receptor. J Biol Chem 281: 15780–15789.

Pontier SM, Percherancier Y, Galandrin S, Breit A, Gales C, Bouvier M (2008). Cholesterol-dependent separation of the beta2-adrenergic receptor from its partners determines signaling efficacy: insight into nanoscale organization of signal transduction. J Biol Chem 283: 24659–24672.

Prinetti A, Loberto N, Chigorno V, Sonnino S (2009). Glycosphingolipid behaviour in complex membranes. Biochim Biophys Acta 1788: 184–193.

Pucadyil TJ, Chattopadhyay A (2004). Cholesterol modulates ligand binding and G-protein coupling to serotonin(1A) receptors from bovine hippocampus. Biochim Biophys Acta 1663: 188–200.

Qanbar R, Bouvier M (2003). Role of palmitoylation/depalmitoylation reactions in G-protein-coupled receptor function. Pharmacol Ther 97: 1–33.

Renner U, Glebov K, Lang T, Papusheva E, Balakrishnan S, Keller B *et al.* (2007). Localization of the mouse 5-hydroxytryptamine(1A) receptor in lipid microdomains depends on its palmitoylation and is involved in receptor-mediated signaling. Mol Pharmacol 72: 502–513.

Rosenbaum DM, Cherezov V, Hanson MA, Rasmussen SG, Thian FS, Kobilka TS *et al.* (2007). GPCR engineering yields high-resolution structural insights into beta2-adrenergic receptor function. Science 318: 1266–1273.

Rozenfeld R, Devi LA (2008). Regulation of CB1 cannabinoid receptor trafficking by the adaptor protein AP-3. FASEB J 22: 2311–2322.

Rybin VO, Xu X, Lisanti MP, Steinberg SF (2000). Differential targeting of beta -adrenergic receptor subtypes and adenylyl cyclase to cardiomyocyte caveolae. A mechanism to functionally regulate the cAMP signaling pathway. J Biol Chem 275: 41447–41457.

Sali A, Blundell TL (1993). Comparative protein modelling by satisfaction of spatial restraints. J Mol Biol 234: 779–815.

Sarnataro D, Grimaldi C, Pisanti S, Gazzerro P, Laezza C, Zurzolo C *et al.* (2005). Plasma membrane and lysosomal localization of CB1 cannabinoid receptor are dependent on lipid rafts and regulated by anandamide in human breast cancer cells. FEBS Lett 579: 6343–6349.

Schroeder H, Leventis R, Rex S, Schelhaas M, Nagele E, Waldmann H *et al.* (1997). S-Acylation and plasma membrane targeting of the farnesylated carboxyl-terminal peptide of N-ras in mammalian fibroblasts. Biochemistry 36: 13102–13109.

Scotter EL, Abood ME, Glass M (2010). The endocannabinoid system as a target for the treatment of neurodegenerative disease. Br J Pharmacol 160: 480–498.

Selent J, Sanz F, Pastor M, De Fabritiis G (2010). Induced effects of sodium ions on dopaminergic G-protein coupled receptors. PLoS Comput Biol doi: 10.1371/journal.pcbi.100088. Available from: http://www.ncbi.nlm.nih.gov/pubmed/20711351.

Shaul PW, Smart EJ, Robinson LJ, German Z, Yuhanna IS, Ying Y *et al*. (1996). Acylation targets emdothelial nitric-oxide synthase to plasmalemmal caveolae. J Biol Chem 271: 6518–6522.

Shrivastava S, Pucadyil TJ, Paila YD, Ganguly S, Chattopadhyay A (2010). Chronic cholesterol depletion using statin impairs the function and dynamics of human serotonin(1A) receptors. Biochemistry 49: 5426–5435.

Smith TH, Sim-Selley LJ, Selley DE (2010). Cannabinoid CB1 receptor-interactinG-proteins: novel targets for central nervous system drug discovery? Br J Pharmacol 160: 454–466.

Song KS, Li S, Okamoto T, Quilliam LA, Sargiacomo M, Lisanti MP (1996). Co-purification and direct interaction of Ras with caveolin, an integral membrane protein of caveolae microdomains. Detergent-free purification of caveolae microdomains. J Biol Chem 271: 9690–9697.

Tanaka K, Nagayama Y, Nishihara E, Namba H, Yamashita S, Niwa M (1998). Palmitoylation of human thyrotropin receptor: slower intracellular trafficking of the palmitoylation-defective mutant. Endocrinology 139: 803–806.

Tian X, Guo J, Yao F, Yang DP, Makriyannis A (2005). The conformation, location, and dynamic properties of the endocannabinoid ligand anandamide in a membrane bilayer. J Biol Chem 280: 29788–29795.

Vogler O, Barcelo JM, Ribas C, Escriba PV (2008). Membrane interactions of G-proteins and other related proteins. Biochim Biophys Acta 1778: 1640–1652.

Wang H, Dey SK, Maccarrone M (2006). Jekyll and Hyde: two faces of cannabinoid signaling in male and female fertility. Endocr Rev 27: 427–448.

Wu B, Chien EY, Mol CD, Fenalti G, Liu W, Katritch V *et al*. (2010). Structures of the CXCR4 chemokine GPCR with small-molecule and cyclic peptide antagonists. Science 330: 1066–1071.

Xiang Y, Rybin VO, Steinberg SF, Kobilka B (2002). Caveolar localization dictates physiologic signaling of beta 2-adrenoceptors in neonatal cardiac myocytes. J Biol Chem 277: 34280–34286.

Xie XQ, Chen JZ (2005). NMR structural comparison of the cytoplasmic juxtamembrane domains of G-protein-coupled CB1 and CB2 receptors in membrane mimetic dodecylphosphocholine micelles. J Biol Chem 280: 3605–3612.

Xu F, Wu H, Katritch V, Han GW, Jacobson KA, Gao ZG *et al*. (2011). Structure of an agonist-bound human A2A adenosine receptor. Science 332: 322–327.

Yamabhai M, Anderson RG (2002). Second cysteine-rich region of epidermal growth factor receptor contains targeting information for caveolae/rafts. J Biol Chem 277: 24843–24846.

Zacharias DA, Violin JD, Newton AC, Tsien RY (2002). Partitioning of lipid-modified monomeric GFPs into membrane microdomains of live cells. Science 296: 913–916.